High-pressure single-crystal X-ray diffraction study of katoite hydrogarnet: Evidence for a phase transition from $Ia3d \rightarrow I\bar{4}3d$ symmetry at 5 GPa

GEORGE A. LAGER,[1,]* ROBERT T. DOWNS,[2] MARCUS ORIGLIERI,[2] AND REBECCA GAROUTTE[2]

[1]Department of Geography and Geosciences, University of Louisville, Louisville, Kentucky 40292, U.S.A.
[2]Department of Geosciences, University of Arizona, Tucson, Arizona 95721, U.S.A.

ABSTRACT

The crystal structure of katoite hydrogarnet has been refined at 0.0001, 2.15, 4.21, 5.09, 6.00, 7.09, and 7.78 GPa from single-crystal X-ray diffraction data using a 4:1 methanol:ethanol mixture as pressure medium in a Merrill-Bassett diamond-anvil cell. Below ~5 GPa, the katoite structure has $Ia3d$ symmetry and compresses by bond shortening rather than bond bending, in agreement with recent quantum mechanical calculations. An unconstrained third-order Birch-Murnaghan fit to the unit-cell volumes and pressures for $Ia3d$ symmetry gave the following equation of state parameters: $V_o = 1987.6(1)$ Å^3, $K_o = 58(1)$ GPa and $K' = 4.0(7)$. Above this pressure, the structure undergoes a phase transition to space group $I\bar{4}3d$, a non-centric subgroup of $Ia3d$. In the $I\bar{4}3d$ structure, there are two non-equivalent (O_4H_4) groups. Both the Ca and Al atoms are displaced along $\boldsymbol{a}$ relative to their positions in $Ia3d$. It is proposed that compression of the short H-H distance between (O_4H_4) groups destabilizes the structure and may initiate the observed phase transition. Corroboration of this model will require accurate information on the hydrogen atom positions at pressures above 5 GPa.

INTRODUCTION

Katoite garnet $[Ca_3Al_2(O_4H_4)_3]$, the Si-free end-member of the hydrogrossular solid-solution series, has received considerable attention in the literature because it is a model for the incorporation of OH in silicate garnets that occur in the Earth's crust and mantle (Lager et al. 1987). The structure and bulk modulus of this garnet ($Ia3d$ symmetry) has recently been determined to 70 GPa using ab initio quantum mechanical calculations (Nobes et al. 2000a, 2000b). It was proposed that bond shortening, as opposed to bond bending, was the primary mechanism of compression. This conclusion was based, in part, on the relative change in the tetrahedral-octahedral rotation angle, which shows only a small variation with pressure. The calculated trend is in agreement with neutron powder diffraction results (Lager and Von Dreele 1996) below 4 GPa but differs in both sign and magnitude from neutron data at higher pressures. If fluorinert is used as the pressure-transmitting medium, it is well known that deviatoric stress in the neutron diffraction experiment can cause significant strain broadening of Bragg reflections and loss of resolution above ~2–3 GPa. In this study, single-crystal X-ray diffraction data were collected to 7.78 GPa to re-examine the compression mechanism based on the neutron data and evaluate the discrepancy between the neutron and theoretical results.

EXPERIMENTAL METHODS

The katoite single crystals were synthesized in a Teflon-lined Parr vessel (~80% filled with H_2O) using a stoichiometric mixture of Al foil (in the form of strips) (Aldrich 35,685-0, 0.05 mm thick, 99.8%) and reagent-grade lime (CaO). After seven days at 423 K, this method produced relatively large single crystals (up to 800 μm) in a matrix of fine-grained material (<10 μm).

A crystal fragment with dimensions $120 \times 100 \times 50$ μm was first examined in air outside the diamond-anvil cell on a Picker automated four-circle diffractometer (45 kV; 40 mA; unfiltered, non-monochromatic Mo$K\alpha$ radiation). Reflection profiles (ω scans) were sharp (FWHM = 0.08°) with no indication of twinning. A small subset of reflections, e.g., (400), showed significant thermal diffuse scattering. Intensity data were collected in air assuming space group symmetry $Ia3d$ and the structure was refined using RFINE4 (Finger and Prince 1975). The unit-cell parameter and atomic coordinates were consistent with the single-crystal X-ray results of Lager et al. (1987) and are not reported in this study.

High-pressure experiments were carried out using a 4-pin Merrill-Bassett diamond-anvil cell with 600 μm culets. The crystal was mounted in a 350 μm diameter sample hole drilled into an Inconel steel gasket (250 μm thickness; preindented to 100 μm) with an electrostatic discharge machine. A 4:1 methanol:ethanol mixture was used as pressure-transmitting medium. The pressure was determined from the shift in the fluorescence lines of a small ruby chip mounted in the sample hole. The R_1 and R_2 peaks at each pressure were fit with Lorentzian functions; pressure was calculated using the relationship given by Mao et al. (1978). Errors in the pressure are estimated to be ±0.05 GPa.

Unit-cell parameters at ten pressures up to 7.78 GPa were determined from least-squares refinement of 25 reflections (8°

* E-mail: galager@louisville.edu

$\leq 2\theta \leq 48°$) using an eight-reflection centering technique (King and Finger 1979) (Table 1). Generally, in a high-pressure experiment, a full sphere of intensity data is collected because of the limited number of reflections accessible through the diamond-anvil cell. However, given the large unit cell of garnet (>3000 reflections), this is impractical because of the diffractometer time required. Hazen and Finger (1989) previously tried to address this problem in their study of andradite and pyrope by including in the data set only those reflections that strongly influenced the variation in structural parameters (leverage analysis). This method requires few high-quality data, and may not be feasible with the diamond-anvil cell because of restricted access to reciprocal space and systematic absorption problems [see, for example, Merli et al. (2000) and references therein]. In this study, a new approach was used. First, all accessible reflections were ordered into equivalence classes. Several symmetry equivalent reflections (usually four) with the lowest diamond-anvil cell absorption were then chosen from each class and used as input to the data-collection routine. In the fixed-ϕ mode that is typically used for single-crystal diffraction experiments at high pressures (Angel et al. 2000), the reflections with the smallest $|\omega|$ values will suffer from the least amount of diamond cell absorption.

Intensity data were collected with ω scans to $\sin\theta/\lambda = 0.7$ Å^{-1} [$2\theta < 60°$] at seven pressures up to 7.78 GPa. Scan width, step size and counting time were $1°$, $0.025°$, and 6s per step, respectively. Each peak was integrated with backgrounds determined by fits to Gaussian functions. Data were corrected for the effects of diamond-anvil cell absorption; symmetry-equivalent reflections were averaged and converted to structure factors using in-house software modified from the suite of programs used at the Geophysical Laboratory. Refinements were carried out with RFINE4. Structure factors were weighted by $[\sigma^2_F + (pF)^2]^{-1}$, where σ_F was obtained from counting statistics and p was chosen to ensure that the errors were normally distributed. It was possible to locate the hydrogen atom in the $Ia3d$ structure and refine its position at high pressure. However, the O-H vector exhibited a significant and non-systematic rotation with pressure, which is chemically unreasonable. As a result, atomic fractional coordinates and anisotropic displacement parameters were refined for all atoms except hydrogen, which was omitted from the refinement models. All refinements below 6.0 GPa converged to weighted R values between 0.020 and 0.034 in space group $Ia3d$. However, the refinement at 6 GPa resulted in a significantly higher R value ($R_w = 0.078$). In addition, the Ca displacement ellipsoid at this pressure became highly anisotropic with the major axis parallel to *a*. A search for all reflections [h, k, $l > 0$] violating $Ia3d$ symmetry revealed weak reflections of the type $hk0$ with $h \neq 2n$, indicating loss of the *a* glide. Multiple diffraction effects were discounted based on the results from ψ scans. Unconstrained unit-cell refinement showed no deviation from cubic geometry. On decompression of the cell to 5.38 GPa, the same $hk0$ reflections were observed but their intensities were significantly weaker (Fig. 1). The pressure was then lowered to 3.08 GPa, and the unit-cell parameter was determined. Reflections violating $Ia3d$ symmetry were not found (Fig. 1). Based on the quality of the refinement at 5.09 GPa, the transition pressure is assumed to lie between 5.09 and 5.38 GPa.

The structures at 6.00, 7.09, and 7.78 GPa were refined in space group $I\bar{4}3d$, a non-centric subgroup of $Ia3d$. Refinement of these structures in $Ia3d$ resulted in systematically high R values (~0.10). In space group $I\bar{4}3d$, the Ca and Al atoms occupy positions [x, 0, 1/4] and [x, x, x], respectively. There are two non-equivalent O and H positions, i.e., two non-equivalent (O$_4$H$_4$) units. The strong pseudosymmetry above the transition pressure resulted in high correlations ($\rho \sim 0.75$) between the fractional coordinates of the two O atoms and between β_{22} and β_{33} of the Ca atom. Attempts to decouple the O positions, e.g., by randomly offsetting the coordinates, or by alternately refining the two positions, were not successful. Refinement results, atomic fractional coordinates, and displacement parameters are given in Tables 2 and 3. Selected interatomic distances and angles, polyhedral volumes, and distortion parameters are presented in Tables 4 and 5.

RESULTS AND DISCUSSION

Hydrogarnet structure

The general formula of hydrogarnet can be represented as [8]X$_3$[6]Y$_2$([4]SiO$_4$)$_{3-x}$(O$_4$H$_4$)$_x$, where the superscripts in brackets refer to the O coordination of the three types of cations in the structure. The O coordination of the X site can be defined as a triangular dodecahedron (distorted cube) that shares two edges with tetrahedra, four with octahedra (Y site), and four with other

TABLE 1. Unit-cell parameter and volume for katoite at pressure

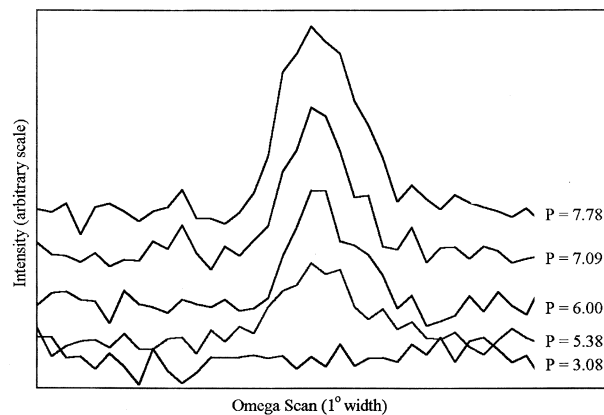| P (GPa)	a (Å)	V (Å^3)
0.0001	12.5731(2)	1987.6(1)
1.24(5)	12.4866(3)	1946.8(1)
2.15(5)	12.4286(3)	1919.8(1)
3.08(5)	12.3719(3)	1893.7(1)
4.21(5)	12.3094(3)	1865.2(1)
5.09(5)	12.2595(3)	1842.5(1)
5.38(5)	12.2442(3)	1835.6(1)
6.00(5)	12.2145(2)	1822.3(1)
7.09(5)	12.1623(4)	1799.0(2)
7.78(5)	12.1267(3)	1783.3(1)

FIGURE 1. Variation in the intensity profiles of the (710) reflection as a function of pressure. Profiles represent ω scans of 1° width, 0.025° step size and 6 s per step counting time.

TABLE 2. Refinement conditions and atom parameters for katoite in $Ia3d$

P(GPa)	0.0001	2.15(5)	4.21(5)	5.09(5)	6.00(5)
R_w	0.032	0.034	0.024	0.018	0.078
p	0.011	0.010	0.0	0.0	0.065
χ	1.13	1.19	1.14	1.17	1.09
No. obs.	250	250	250	248	247
Ca $\beta(1,1)$	0.0021(1)	0.0021(1)	0.0027(1)	0.0034(1)	0.0040(1)
Ca $\beta(2,2)$	0.00151(7)	0.00125(7)	0.00148(6)	0.00163(6)	0.0015(1)
Ca $\beta(2,3)$	0.0000(1)	0.0001(1)	0.0002(1)	−0.0001(1)	−0.0004(1)
B_{so}	1.09(3)	0.95(3)	1.14(2)	1.33(2)	1.41(2)
Al $\beta(1,1)$	0.00138(7)	0.00133(7)	0.00144(6)	0.00172(7)	0.0019(2)
Al $\beta(1,2)$	−0.0000(1)	0.0001(1)	0.0000(1)	0.0001(1)	0.0002(2)
B_{so}	0.88(2)	0.82(2)	0.87(1)	1.03(1)	1.13(3)
O x	0.0285(2)	0.0289(2)	0.0299(2)	0.0306(2)	0.0310(4)
y	0.0522(2)	0.0530(2)	0.0529(2)	0.0528(2)	0.0527(4)
z	0.6402(3)	0.6410(2)	0.6414(2)	0.6421(2)	0.6423(4)
$\beta(1,1)$	0.0026(3)	0.0023(3)	0.0025(2)	0.0028(3)	0.0026(4)
$\beta(2,2)$	0.0020(2)	0.0022(2)	0.0019(2)	0.0023(2)	0.0022(4)
$\beta(3,3)$	0.0016(2)	0.0013(2)	0.0016(2)	0.0020(2)	0.0019(4)
$\beta(1,2)$	−0.0001(2)	−0.0004(2)	−0.0003(1)	−0.0003(1)	−0.0005(3)
$\beta(1,3)$	0.0001(2)	−0.0001(1)	−0.0002(1)	−0.0005(1)	0.0002(3)
$\beta(2,3)$	−0.0002(2)	−0.0002(2)	−0.0003(1)	−0.0003(2)	−0.0004(3)
B_{so}	1.31(7)	1.20(6)	1.21(5)	1.41(6)	1.4(1)

Note: The Ca atom is located at [1/8, 0, 1/4], with $\beta(3,3) = \beta(2,2)$, $\beta(1,2) = \beta(1,3) = 0$; the Al atom is located at [0, 0, 0], with $\beta(1,1) = \beta(2,2) = \beta(3,3)$, $\beta(1,2) = \beta(1,3) = \beta(2,3)$.

TABLE 3. Refinement conditions and atom parameters for katoite in $I\bar{4}3d$

P(GPa)	6.00(5)	7.09(5)	7.78(5)
R_w	0.050	0.023	0.021
p	0.030	0.0	0.010
χ	1.15	1.12	1.06
No. obs.	495	478	474
Ca x	0.1342(3)	0.1354(3)	0.1370(2)
Ca $\beta(1,1)$	0.0022(2)	0.0022(2)	0.0016(2)
Ca $\beta(2,2)$	0.0012(2)	0.0015(2)	0.0014(2)
Ca $\beta(3,3)$	0.0019(2)	0.0016(2)	0.0015(2)
Ca $\beta(2,3)$	−0.0000(1)	0.0004(1)	0.0004(1)
B_{so}	1.08(4)	1.03(4)	0.88(4)
Al x	0.0024(4)	0.0039(3)	0.0032(3)
Al $\beta(1,1)$	0.00163(8)	0.00118(8)	0.00127(7)
Al $\beta(1,2)$	−0.0000(1)	−0.0003(1)	−0.0001(1)
B_{so}	0.97(2)	0.70(2)	0.75(1)
O1 x	0.0339(6)	0.0340(5)	0.0356(5)
y	0.0510(8)	0.0533(5)	0.0528(5)
z	0.6381(8)	0.6386(5)	0.6388(5)
$\beta(1,1)$	0.0012(5)	0.0023(4)	0.0021(4)
$\beta(2,2)$	0.0029(6)	0.0013(4)	0.0016(4)
$\beta(3,3)$	0.0018(6)	0.0013(5)	0.0014(5)
$\beta(1,2)$	−0.0005(4)	−0.0001(4)	−0.0007(3)
$\beta(1,3)$	0.0005(4)	−0.0008(4)	0.0002(3)
$\beta(2,3)$	0.0001(4)	0.0004(3)	0.0002(3)
B_{so}	1.2(1)	1.0(1)	1.0(1)
O2 x	0.1465(9)	0.1468(6)	0.1476(5)
y	0.9717(7)	0.9719(6)	0.9732(5)
z	0.0536(7)	0.0518(5)	0.0538(5)
$\beta(1,1)$	0.0018(5)	0.0014(5)	0.0017(4)
$\beta(2,2)$	0.0044(7)	0.0029(5)	0.0027(5)
$\beta(3,3)$	0.0016(6)	0.0030(4)	0.0019(4)
$\beta(1,2)$	0.0003(5)	−0.0009(4)	0.0001(4)
$\beta(1,3)$	−0.0006(4)	−0.0004(4)	−0.0008(3)
$\beta(2,3)$	0.0001(5)	−0.0003(4)	−0.0002(4)
B_{so}	1.6(2)	1.4(1)	1.2(1)

Note: The Ca atom is located at [x, 0, 1/4], with $\beta(1,2) = \beta(1,3) = 0$; Al is located at [$x$, x, x], with $\beta(1,1) = \beta(2,2) = \beta(3,3)$, $\beta(1,2) = \beta(1,3) = \beta(2,3)$.

TABLE 4. Selected interatomic distances and angles for katoite in $Ia3d$

P(GPa)	0.0001	2.15(5)	4.21(5)	5.09(5)
Ca1-O1	2.462(3)	2.434(3)	2.417(3)	2.410(3)
Ca2-O4	2.520(3)	2.482(3)	2.463(2)	2.455(3)
Mean	2.491	2.459	2.440	2.429
V(CaO$_8$)	25.96	24.97	24.41	24.22
Al-O	1.914(3)	1.906(3)	1.895(3)	1.896(2)
O1···O4	2.599(5)	2.587(5)	2.583(4)	2.593(3)
O1···O5	2.813(6)	2.801(6)	2.772(4)	2.767(5)
V(AlO$_6$)	9.28	9.15	9.00	9.03
Angle Var.*	22.47	22.59	17.84	14.85
d1-O†	1.952(3)	1.922(3)	1.893(3)	1.873(2)
O1···O2	3.057(6)	3.013(6)	2.974(5)	2.945(4)
O1···O3	3.250(5)	3.201(5)	3.147(4)	3.114(4)
Angle Var.*	24.67	24.21	21.22	20.50
V(dO$_4$)	3.78	3.61	3.45	3.35
d-O-Al	130.7(2)	130.3(2)	130.6(1)	130.8(2)

* Bond angle variance as defined by Robinson et al. (1971).
† d is Wyckoff notation for the position with point symmetry $\bar{4}$ in space group $Ia3d$ (occupied by Si at [3/8,0,1/4] in silicate garnets).

TABLE 5. Selected interatomic distances and angles for katoite in $I\bar{4}3d$

P (GPa)	6.00(5)	7.09(5)	7.78(5)
Ca1-O4a	2.366(9)	2.350(8)	2.340(7)
Ca1-O4a	2.443(9)	2.434(7)	2.432(6)
Ca2-O4a	2.428(9)	2.438(7)	2.405(6)
Ca2-O4b	2.481(10)	2.445(8)	2.450(7)
Mean	2.430	2.417	2.407
V(CaO$_8$)	24.11	23.74	23.42
Al-O1	1.877(9)	1.873(7)	1.891(7)
Al-O2	1.905(10)	1.904(6)	1.892(6)
Mean	1.891	1.888	1.892
O1···O4	2.573(17)	2.571(10)	2.590(11)
O1···O5	2.730(10)	2.709(7)	2.720(7)
V(AlO$_6$)	8.96	8.92	8.97
Angle Var*	12.53	15.76	15.08
d1-O†	1.869(10)	1.866(6)	1.845(7)
O1a···O2a	3.004(22)	3.004(11)	2.986(13)
O1a···O3a	3.077(16)	3.068(10)	3.026(11)
V(dO$_4$)	3.35	3.33	3.22
Angle Var*	3.88	3.04	1.27
d-O-Al	132.5(6)	130.4(3)	131.5(3)
d2-O	1.850	1.833(7)	1.840(7)
O1b···O2b	2.847(22)	2.809(14)	2.805(14)
O1b···O3b	3.104(17)	3.082(13)	3.100(12)
V(dO$_4$)	3.19	3.10	3.12
Angle Var*	48.05	55.42	63.44
d-O-Al	129.9(5)	131.4(4)	129.4(3)

* Bond angle variance as defined by Robinson et al. (1971).
† d is Wyckoff notation for the position with point symmetry $\bar{4}$ in space group $Ia3d$ (occupied by Si in silicate garnets); d1 and d2 are located at [3/8,0,1/4] and [3/4,5/8,0], respectively, in space group $I\bar{4}3d$.

dodecahedra. The dodecahedral cavities are located within a framework composed of corner sharing octahedra and tetrahedra (Novak and Gibbs 1971). When Si does not occupy the tetrahedron, each O atom surrounding the vacancy is bonded to an H atom. In space group $Ia3d$, the hydrogarnet structure is uniquely defined by the fractional coordinates of the O and H atoms and by the unit-cell parameter. The cation positions are fixed by symmetry. As noted above, there are two non-equivalent O and H positions and two non-equivalent (O$_4$H$_4$) tetrahedra in space group $I\bar{4}3d$. One tetrahedron is quite regular (d1) whereas the other is distorted (d2) (Table 5). Just above the transition pressure the Ca atom is displaced by 0.112 Å along **a** in the direction of d1, which has the longer shared edge (Table 5). The Al atom is also displaced relative to its position in $Ia3d$ and moves 0.051 Å along the threefold axis.

Bulk modulus

An unconstrained third-order Birch-Murnaghan fit to the unit-cell volumes and pressures for $Ia3d$ symmetry gave the following equation of state parameters: $V_o = 1987.6(1)$ Å^3, $K_o = 58(1)$ GPa, and $K' = 4.0(7)$ (Table 1; Fig. 2). This value of the bulk modulus lies between the experimental data of Olijnyk et al. (1991) [$K_o = 66(4)$ GPa] and Lager and Von Dreele (1996) [$K_o = 52(1)$ GPa] and is within two estimated standard deviations of the theoretical value calculated by Nobes et al. (2000a, 2000b) [$K_o = 56.2(1.2)$ GPa] (Fig. 2). The unit-cell volumes calculated from the quantum mechanical model are systematically higher (~1–2%) than those observed experimentally, as shown in Figure 2.

In the Olijnyk et al. (1991) study to 42 GPa, K_o was determined using pressure media (alcohol, nitrogen) that freeze and become non-hydrostatic above 10 GPa. In addition, the unit-cell parameter was calculated from only four reflections fit with pure Gaussian profiles. The bulk modulus determined by Lager and Von Dreele (1996) should, in principle, be more accurate than the X-ray powder value because it was derived from a fit to the whole neutron powder spectrum using the Rietveld method; however, as discussed by these authors, neutron powder data can also be affected by deviatoric stress. The K_o value in this study was determined from data below 6 GPa and extrapolated to higher pressure, as indicated by the dashed line in Figure 2. An examination of Figure 2 shows that there is no apparent volume discontinuity at the transition pressure. If the bulk modulus is computed based on the complete pressure-volume (PV) data in Table 1, then $V_o = 1987.6(1)$ Å^3, $K_o = 57.9(7)$ GPa, and $K' = 4.0(3)$.

Variation in structural parameters at high pressure

Below the phase transition, the largest variations in the O atom positional parameters are observed in the x and z coordi-
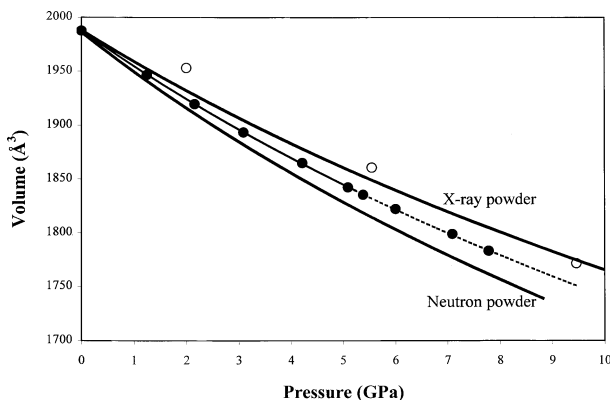

FIGURE 2. Comparison of the pressure dependence of the unit-cell volume for the X-ray powder data (Olijnyk et al. 1991), neutron powder data (Lager and Von Dreele 1996), and the single-crystal X-ray data determined in this study (solid circles). The solid curve represents the fit to the PV data for $Ia3d$ katoite [$K_o = 58(1)$ GPa and $K' = 4.0(7)$]. The dashed line has been extrapolated from this fit. Unit-cell volumes calculated by Nobes et al. (2000a, 2000b) are represented by open circles.

nates. The y coordinate, which is related to rigid body rotations of the octahedra and tetrahedra, remains relatively constant. In fact, there is no significant change in the tetrahedral-octahedral (d-O-Al) angle indicating that bond bending is not an important compression mechanism in $Ia3d$ katoite (Table 4), in agreement with the theoretical results (Nobes et al. 2000a, 2000b). The neutron powder data (Lager and Von Dreele 1996) show a similar variation over this low-pressure range. This behavior is in contrast to that observed in silicate garnets pyrope and grossular, where the Si-O-Al angle varies in response to changes in the tilt and distortion of the tetrahedra and octahedra (Hazen and Finger 1989; Zhang et al. 1998). Above 6 GPa, it is difficult to make comparisons among these studies because the phase transition was not observed in the neutron data and the theoretical calculation assumed $Ia3d$ symmetry.

The pressure dependence of the polyhedral volumes is shown in Figure 3. Polyhedral bulk moduli are generally consistent with those determined in the neutron powder (Lager and Von Dreele 1996) and theoretical studies (Nobes et al. 2000a, 2000b). Based on PV data below the transition, K_o values decrease in the order AlO$_6$ [$K_o = 153(2)$ GPa; $K' \equiv 4$] > CaO$_8$ [$K_o = 61(2)$; $K' \equiv 4$] > O$_4$H$_4$ [$K_o = 35(2)$; $K' \equiv 4$]. As noted in these previous studies, the bulk modulus of the Ca dodecahedron is approximately equal to the bulk modulus of the crystal. The lower bulk modulus of katoite relative to that observed in silicate garnets (e.g., for grossular, $K_o = 175(1)$; Zhang et al. 1999) can be attributed primarily to the higher compressibilities of the Ca dodecahedron and (O$_4$H$_4$) tetrahedron. The quantum mechanical study predicts a stiffer Al octahedron (196 GPa) and a softer (O$_4$H$_4$) tetrahedron (19 GPa) relative to the experimental studies. The theoretical value for the bulk modulus of the Al octahedron is similar to that observed in pyrope (211 GPa; Zhang et al. 1998) and grossular (220 GPa; Hazen and Finger 1978).

A close examination of the variations in interatomic distances and angles with pressure does not reveal an obvious mechanism for the phase transition, i.e., no unrealistically short bond distances or polyhedral distortions develop at pressure. Unfortunately, the X-ray refinements provided limited information on the hydrogen atoms, which likely play a pivotal role in the transition.

Re-examination of the neutron powder diffraction results

In the high-pressure neutron study, Lager and Von Dreele (1996) observed a significant compression of the O-D bond length, which is inconsistent with results from spectroscopic measurements (Knittle et al. 1992) and ab initio calculations (Nobes et al. 2000a, 2000b). Both of these studies suggest that the O-H(D) bond remains essentially constant in length over the pressure range examined in the neutron experiment. If one considers the neutron data up to 6.1 GPa, the O-D bond length decreases from 0.906(2) Å at ambient pressure to 0.862(15) Å at 6.1 GPa. Lager and Von Dreele (1996) proposed that the shortening of the O-D bond could be related to D-D repulsion between adjacent OD groups in the (O$_4$D$_4$) tetrahedron as the O···O distances compress. The D-D distance in katoite, which is less than the sum of the van der Waals radii of H at ambient pressure [1.956(2)], decreases to 1.76(3) Å at 6.1 GPa (Lager

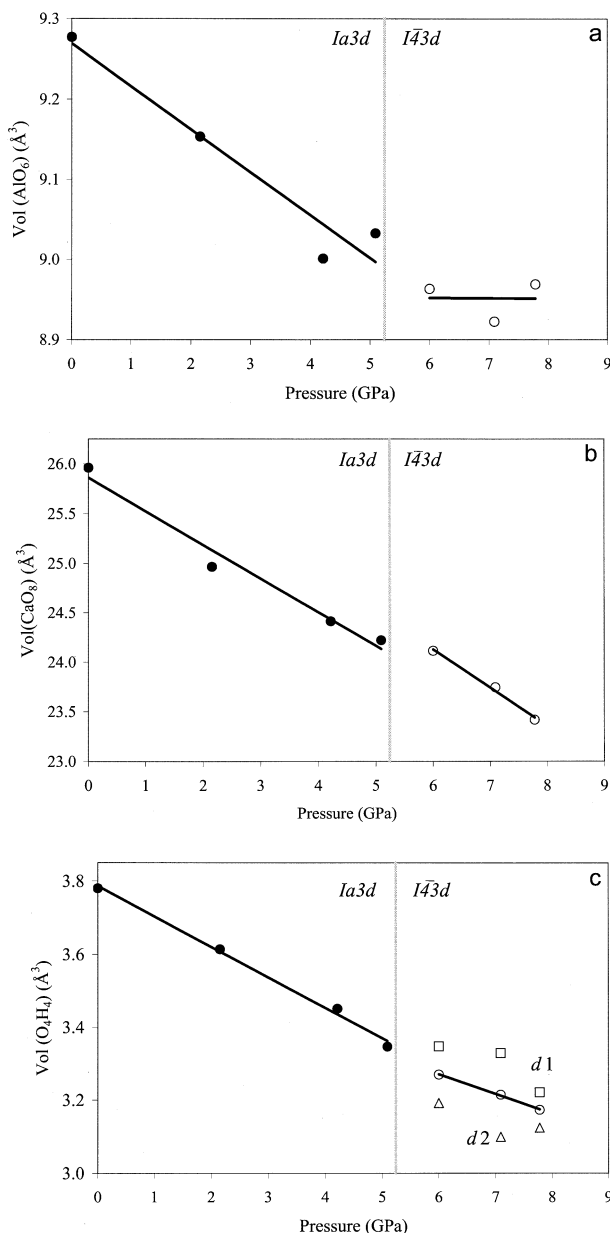**FIGURE 3.** Plots of the AlO_6 (**a**), CaO_8 (**b**), and O_4H_4 (**c**) polyhedral volumes vs. pressure for katoite. Solid circles represent values from $Ia3d$ structure; open circles represent $I\bar{4}3d$. In the case of the tetrahedral volume, open circles represent the average value. Solid lines represent best fits meant to aid the eye.

sure range of this study. The smallest displacement amplitude of the D atom is parallel to the O-D bond and is approximately equal to the amplitude of the O atom in the same direction. Therefore, the riding model (Busing and Levy 1964) can be used to describe the correlated thermal motion of the O and D atoms. Application of the simple riding model (Downs et al. 1992) to the O-D bond length in katoite at ambient pressure yields a corrected distance of 0.94 Å, a value that is in better agreement with the mean O-D distance [0.969(1) Å; Ceccarelli et al. 1981] determined from numerous neutron diffraction studies. Neutron data at T = 100 and 200 K (Lager et al. 1987) are also consistent with the riding model, thus establishing that the displacement factors of the D atoms in katoite reflect true thermal motion and not static disorder.

Anisotropic displacement parameters were not determined for the high-pressure neutron data; however, the sample used in that experiment was exactly the same as in the low-temperature study. Therefore, it is assumed that the riding model can be applied to the high-pressure data. Although anisotropic displacement parameters are needed to establish the validity of the riding model, the correction can be computed with isotropic parameters using the simple riding model that was developed by Downs et al. (1992). The displacement parameters of D in the high-pressure neutron study increase from B_{eq} = 3.1(5) Å^2 at ambient pressure to B_{eq} = 4.2(6) Å^2 at 6.1 GPa. Application of this simple riding model uniformly produces corrected O-D bond distances of 0.94 Å, suggesting that the apparent shortening of the O-D distance in this pressure range may be due only to the effects of thermal motion. The increase in thermal amplitudes of D with pressure is consistent with, and may be caused by, the decrease in the tetrahedral volume at high pressure.

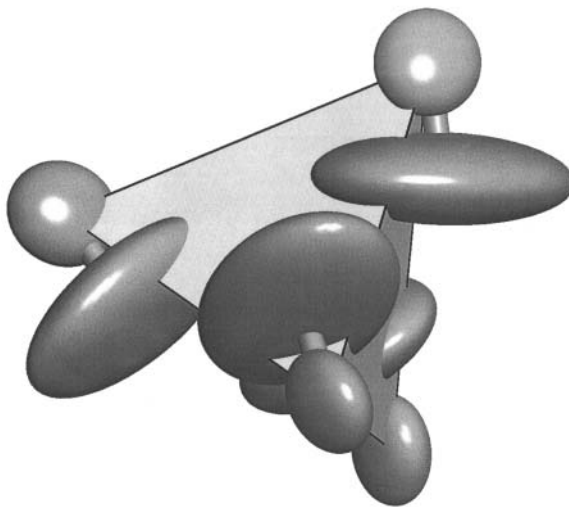Figure 5 illustrates two adjacent (O_4D_4) tetrahedra in katoite

FIGURE 4. Structure drawing of O_4D_4 tetrahedron at 295 K and ambient pressure based on the neutron powder data of Lager et al. (1987). Displacement ellipsoids of O and D are drawn at 99.99% probability. Note that the equal amplitudes of O and D along the O-D vector satisfy the riding model criterion and that the vibrations of the D atoms penetrate the tetrahedron.

and Von Dreele 1996).

The short D-D distance in the (O_4D_4) tetrahedron in katoite at ambient pressure (Lager et al. 1987) is highlighted in Figure 4. It can be seen that the displacement of the D atom is strongly anisotropic with the largest amplitude oriented approximately perpendicular to the O-D bond and toward the inside of the tetrahedron. All four D atoms vibrate into the tetrahedron, thus requiring a highly correlated motion, which is consistent with the thermal diffuse scattering observed throughout the pres-

at ambient pressure. The size of the D displacement ellipsoids has been drawn at 99.99% probability to show the orientations of the ellipsoids in the short, *inter-polyhedral* D-D distance. Note that the displacement ellipsoids point toward one another producing an overlap, which is not observed within the tetrahedron (Fig. 4). The tetrahedra illustrated in Figure 5 are symmetry equivalent in space group $Ia3d$; however, they become non-equivalent in $I\bar{4}3d$. It is proposed that compression of this short D-D distance at high pressure may destabilize the structure and initiate the phase transition from $Ia3d$ to $I\bar{4}3d$. The inter-polyhedral D-D distance becomes shorter than the intra-polyhedral distance at about 5 GPa in the ab initio study but remains relatively constant with pressure in the neutron study (~2 Å). Without accurate positions for H above the transition pressure, however, it is difficult to corroborate this model.

There were no violations of space group symmetry $Ia3d$ observed above 5 GPa in the neutron powder spectra. This could be due to the peak broadening at high pressures, and to the fact that all $(hk0)$ peaks that established $I\bar{4}3d$ symmetry overlap with peaks found in $Ia3d$. Nevertheless, based on the results of this study, an attempt was made to refine the neutron structure above 5 GPa in space group $I\bar{4}3d$. The refinement was initiated with the X-ray positions for the non-D atoms. One deuterium position (D1) should be similar to that determined by Lager et al. (1987); the starting value for second position (D2) was determined from the list of 96 sites possible in space group $Ia3d$ after excluding all symmetry equivalent positions of D1. The refinement was ill-behaved and did not converge when all atomic coordinates were varied simultaneously. Because strain broadening of the neutron spectrum becomes appreciable near the transition pressure, the quality of the neutron powder data is probably not adequate to resolve the small differences between refinement models.

REFERENCES CITED

Angel, R.J., Downs, R.T., and Finger, L.W. (2000) High-temperature–high-pressure diffractometry. In R.M. Hazen and R.T. Downs, Eds., High-Temperature and High-Pressure Crystal Chemistry, 41, p. 559–596. Reviews in Mineralogy and Geochemistry, Mineralogical Society of America, Washington, D.C.

Busing, W.R. and Levy, H.A. (1964) The effect of thermal motion on the estimation of bond lengths from diffraction measurements. Acta Crystallographica, 17, 142–146.

Ceccarelli, C., Jeffrey, G.A., and Taylor, R. (1981) A survey of O-H···O hydrogen bond geometries determined by neutron diffraction. Journal of Molecular Structure, 70, 255–271.

Downs, R.T., Gibbs, G.V., Bartelmehs, K.L., and Boisen, M.B. Jr. (1992) Variations of bond lengths and volumes of silicate tetrahedra with temperature. American Mineralogist, 77, 751–757.

Finger, L.W. and Prince, E. (1975) A system of Fortran IV computer programs for crystal structure computations. United States National Bureau of Standards, Technical Note 854, 128 p.

Hazen, R.M. and Finger, L.W. (1978) Crystal structures and compressibilities of pyrope and grossular to 60 kbar. American Mineralogist, 63, 297–303.

———(1989) High-pressure crystal chemistry of andradite and pyrope: Revised procedures for high-pressure diffraction experiments. American Mineralogist, 74, 352–359.

King, H.E. and Finger, L.W. (1979) Diffracted beam crystal centering and its application to high-pressure crystallography. Journal of Applied Crystallography, 12, 374–378.

Knittle, E., Hathorne, A., Davis, M., and Williams, Q. (1992) A spectroscopic study of the high-pressure behavior of the O_4H_4 substitution in garnet. In Y. Syono and M.H. Manghnani, Eds., High-pressure research: Application to earth and planetary Sciences, 67, p. 297–304.Geophysical Monograph, American Geophysical Union, Washington, D.C.

Lager, G.A., Armbruster, T., and Faber, J. (1987) Neutron and X-ray diffraction study of hydrogarnet $Ca_3Al_2(O_4H_4)_3$. American Mineralogist, 72, 756–765.

Lager, G.A. and Von Dreele, R.B. (1996) Neutron powder diffraction of hydrogarnet to 9.0 GPa. American Mineralogist, 81, 1097–1104.

Mao, H.K., Bell, P.M., Shaner, J.W., and Steinberg, D.J. (1978) Specific volume measurements of Cu, Mo, Pd, and Ag and calibration of the ruby R_1 fluorescence pressure gauge from 0.06 to 1 Mbar. Journal of Applied Physics, 49, 3276–3283.

Merli, M., Ungaretti, L., and Oberti, R. (2000) Leverage analysis and structure refinement of minerals. American Mineralogist, 85, 532–542.

Novak, G.A. and Gibbs, G.V. (1971) The crystal chemistry of the silicate garnets. American Mineralogist, 56, 791–825.

Nobes, R.H., Akhmatskaya, E.V., Milman, V., White, J.A., Winkler, B., and Pickard, C.J. (2000a) An ab initio study of hydrogarnets. American Mineralogist, 85, 1706–1715.

Nobes, R.H., Akhmatskaya, E.V., Milman, V.,Winkler, B., and Pickard, C.J. (2000b) Structure and properties of aluminosilicate garnets and katoite: an ab initio study. Computational Materials Science, 17, 141–145.

Olijnyk, H., Paris, E., Geiger, C.A., and Lager, G.A. (1991) Compressional study of katoite [$Ca_3Al_2(O_4H_4)_3$] and grossular garnet. Journal of Geophysical Research, 96, 14,313–14,318.

Robinson, K., Gibbs, G.V., and Ribbe, P.H. (1971) Quadratic elongation: A quantitative measure of distortion in coordination polyhedra. Science, 172, 567–570.

Zhang, L., Ahsbahs, H., and Kutoglu, A. (1998) Hydrostatic compression and crystal structure of pyrope to 33 GPa. Physics and Chemistry of Minerals, 25, 301–307.

Zhang, L., Ahsbahs, H., Kutoglu, A., and Geiger, C.A. (1999) Single-crystal hydrostatic compression of synthetic pyrope, almandine, spessartine, grossular and andradite garnets at high pressures. Physics and Chemistry of Minerals, 27, 52–58.
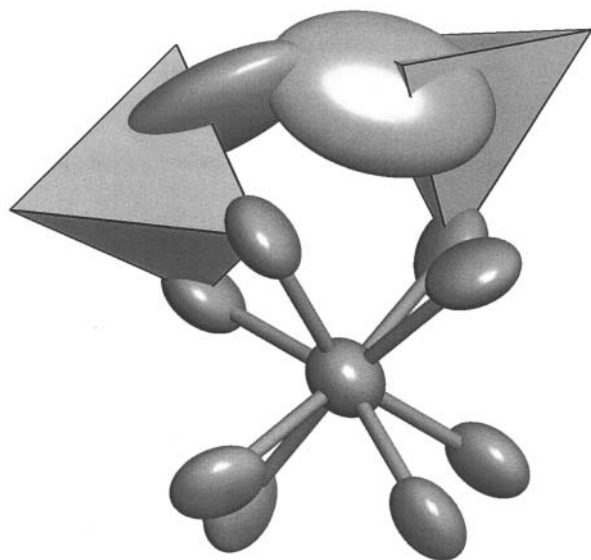

FIGURE 5. Structure drawing of adjacent O_4D_4 tetrahedra and CaO_8 group at 295 K and ambient pressure based on the neutron powder data of Lager et al. (1987). Displacement ellipsoids are drawn at 99.99% probability. Note that the displacement ellipsoids of the D atoms overlap. It is proposed that this overlap destabilizes the structure at high pressure and may initiate the observed phase transition.